

INFLUENCE OF ALBUMIN ADSORPTION ON PHYSICO-CHEMICAL PROPERTIES OF ALUMINA SURFACES

D. Sternik, P. Staszczuk*, J. Sobieszek, M. Płanda-Czyż and S. Wasak

Department of Physicochemistry of Solid Surface, Chemistry Faculty, Maria Curie-Skłodowska University
M. Curie-Skłodowska Sq. 3, 20-031 Lublin, Poland

The effect of albumin adsorption on neutral active aluminium oxide was investigated in the presence of polar and non-polar liquids. The adsorbed values were highest near the isoelectric point of albumin and varied in the range 5–10 and 3–11 mg g⁻¹ with phosphate buffer and potassium chloride respectively after 2 and 24 h. In the case of aluminium oxide the effect of albumin adsorption on total heterogeneity of adsorbents is not explicit. On the one hand, the modified samples showed decreasing surface area with increase of surface coverage with albumin. On the other hand, modifications under the same conditions but without albumin caused similar changes. These effects suggest the strong influence of medium pH on surface properties (due to surface polarization) and competitive co-adsorption of ions on the process. The volumetric fractal dimensions of the studied materials change in the range 2.25–2.32 for pure aluminium oxide and BSA modified from the phosphate solution. $E_{d,max}$ values (desorption energy in the maximum of distribution function) diminish (in the range 40–45 kJ mol⁻¹) compared with pure aluminium oxide ($E_{d,max}=52$ kJ mol⁻¹) for water thermodesorption at modified surfaces to the increase of a number of active centers of hydrophobic character, and weakening of the adsorbent–adsorbate increases.

Keywords: albumin adsorption, aluminium oxide, desorption energy, fractal dimensions, total heterogeneity

Introduction

Solid materials, such as aluminium oxide, are important because of their adsorbent properties, resulting in their potential applications [1–7]. The properties of solid surfaces strongly depend on the number and nature of surface-active centres as well as on porosity: specific surface area, pore volume and pore-size distribution function. The different characteristics of active centres on the surface of alumina are various. For example, there are strong electric fields in places on the alumina [8]. These result mainly from basic ions (O²⁻), acidic ions (Al³⁺) and electron-acceptor surface defects; there are also hydroxyl groups formed, responsible for their amphoteric character [9–12].

The mechanisms of interactions of proteins with adsorbents vary widely: Lewis acid-base force, Lifshits–van der Waals force, electrostatic force, hydrophobic effect, etc. The adsorption of albumin from solution depends on surface and environment properties [13–17]. Despite the extensive studies of albumin adsorption, there is little information on the total heterogeneity (geometrical and energetical) of the solid surfaces modified by proteins, which are used for production of biosensor and chiral stationary phases.

Many complex methods have been applied to the investigation of protein, protein/liquid and protein/solid systems [18–24]. For instance, for determining the

amount adsorbed: spectroscopic methods (ultraviolet, Bradford, Lowery, BCA, ellipsometry, infrared) or elemental analysis, to determine conformations of protein: nuclear magnetic resonance, circular dichroism (CD), differential scanning calorimetry (DSC), Raman and IR spectroscopy, to determine physico-chemical properties protein and protein/solid systems: thermal analysis, sorptometry and porosimetry, liquid chromatography and microscopy.

The paper presents the description of differences in physicochemical properties of mesoporous adsorbents with physically bonded albumins. The mechanism of adsorption–desorption of albumin from non-porous alumina samples was presented in literature [25, 26]. The properties of solid surfaces strongly depend on the number and nature of surface active centres as well as on porosity: specific surface area, pore volume and pore-size distribution function. The effect of modification on surface parameters of alumina is discussed.

Experimental

Materials

Albumin bovine (BSA, Fraction V, minimum 98%) and ovalbumine were purchased from Sigma. Neutral active alumina was obtained from Merck. All other reagents were analytical grade.

* Author for correspondence: piotr@hermes.umcs.lublin.pl

Modification

The active alumina oxide (fraction 0.06–0.1 mm) was dried at 200°C for 5 h. Albumin (BSA and ovalbumin) stock solution (8 cm³, 1.4 mg cm⁻³ concentration and determined pH, based on phosphate buffer or KCl solution) and alumina (0.5 g) were added to plastic reactors. The mixtures were precipitated at 25°C with 120 rpm for 2 or 24 h. Then the adsorbent was separated from the solution, washed with buffer solution, dried at room temperature in a desiccator with molecular sieves for 3 days and heated at 45°C for 24 h. The solution was centrifuged and adsorbed protein concentration was determined (by the difference in absorbance before and after modification at $\lambda=279$ nm). Phosphate buffer (Ph) was prepared using Na₂HPO₄ (0.05 M) and NaH₂PO₄ (0.05 M) solution to obtain a given pH value. The solutions based on KCl of a determined pH value were prepared from KOH or HCl solutions (0.01 M) and KCl solution (0.1 M).

Methods

Polar (water) and non-polar (octane) liquids thermodesorption from the synthesized material surface was studied using an apparatus of Q-1500D type (MOM, Hungary). The samples were saturated with liquid vapour in a vacuum desiccator where $p/p_0=1$ for 48 h to establish the state of liquid adsorption equilibrium. The gel samples were removed to the measuring crucible placed in the furnace of derivatograph and 3 measurements were made in the temperature range 20–250°C with a heating rate 6°C min⁻¹. Measurements close to the average value were taken for calculations.

The amount of reacted modifier was determined by the UV-Vis spectrophotometry. Specific surface areas and pore volume were determined by low-temperature nitrogen adsorption (sorptomat ASAP 2405 V1.01) and fractal dimensions were then calculated. Based on the above experimental data, adsorption capabilities as well as total surface heterogeneity of the studied samples were determined and images of the surface were made by atomic force microscopy, AFM (Digital Instruments Nanoscope).

Results and discussion

Structural parameters of the samples determined from the nitrogen adsorption-desorption isotherms are presented in Tables 1 and 2. Examples nitrogen sorption isotherms are presented in Fig. 1. All the isotherms are of type II in accordance with multi-layer nitrogen adsorption. The presence of hysteresis loops on the isotherms points to the capillary phenomenon. In the case of modification with BSA and ovalbumin two effects are observed. On one hand, the effect of size and nature of albumin is observed. Due to small pore sizes, this factor is insignificant (sieve effects). On the other hand, this process is determined by modification time, nature and pH of solution. The BSA adsorbed values are largest near the isoelectric point of albumin as shown in the table (in the range 5–10 and 3–11 mg g⁻¹ after 2 and 24 h for phosphate buffer and potassium chloride, respectively). Only in the case of ovalbumin adsorption from the neutral phosphate solution, the amount of adsorbed albumin in the time did not increase.

The larger amount of proteins results in the decrease of specific surface area of the material (in most cases) as well as of volume and diameter of pores compared with the starting material. This is due to coarseness of sample and is greater in the case of adsorption from phosphate solutions. This process is complicated and ambiguous. In the case of aluminium oxide modification with analogous solutions of phosphate salts and KCl (without albumin) similar changes of sample porosity were obtained. These effects are due to the amphoteric character of the studied material surface and competitive co-adsorption of ions from the solution.

From the adsorption-desorption isotherms of nitrogen, fractal dimensions were calculated from the dependence [27]:

$$D_f = 3 - d[\ln a(x)] / d[\ln(-\ln x)] \quad (1)$$

where a – the adsorption value, $x=p/p_0$.

The volumetric fractal dimensions of the studied materials change in the range 2.26–2.32 for pure aluminium oxide and BSA modified from the phosphate solution. Figure 2 presents the AFM photographs of

Table 1 Adsorption and structural parameters of the pure and modified alumina samples determined from the nitrogen adsorption isotherms

t_{mod}/h	Sample	$S_{\text{BET}}/\text{m}^2 \text{g}^{-1}$	$V_{\text{ads}}/\text{m}^3 \text{g}^{-1}$	$V_{\text{des}}/\text{m}^3 \text{g}^{-1}$	D_{AV}/nm	$D_{\text{N-N}_2}$	$D_{\text{fp-AFM}}$
–	Al ₂ O ₃	188.6	0.23	0.22	4.61	2.26	2.66
2	Al ₂ O ₃ -Ph-pH 4.9	161.6	0.21	0.20	4.76	2.26	
2	Al ₂ O ₃ -Ph-pH 7	164.0	0.22	0.21	4.88	2.27	
24	Al ₂ O ₃ -Ph-pH 4.9	153.3	0.21	0.19	4.81	2.28	2.66
24	Al ₂ O ₃ -Ph-pH 7	157.1	0.21	0.20	4.94	2.27	2.56
24	Al ₂ O ₃ -KCl-pH 4.9	184.9	0.23	0.21	4.48		2.42
24	Al ₂ O ₃ -KCl-pH 7	184.3	0.23	0.21	4.55		

t_{mod} – modification time, S_{BET} – specific surface area, V_{BH} – the pore volume, D_{AV} – pore diameter, D_{N} – volume, D_{fp} – surface fractal dimensions

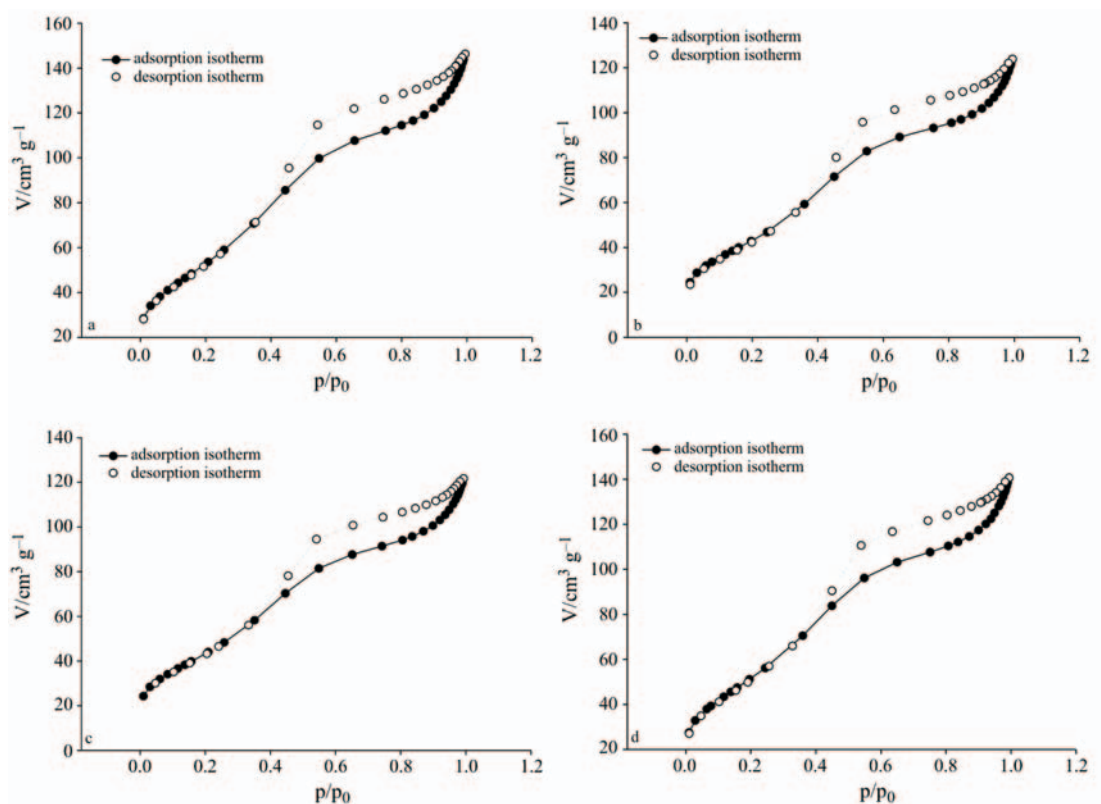


Fig. 1 Examples of nitrogen adsorption–desorption isotherms with unmodified and modified surfaces; a – pure Al_2O_3 , b – Al_2O_3 –24 h–phosphate buffer–pH 4.9, c – Al_2O_3 –24 h–BSA–phosphate buffer–pH 4.9, d – Al_2O_3 –24 h–KCl solution–pH 4.9

the sample surface. The alumina modification causes changes in surface fractal dimensions (D_{fp}) depending on pH and acidity stabilizer (Tables 1 and 2).

Based on the data from thermal analysis, adsorption capacities and a statistical number of monolayers were calculated and present in Fig. 3. From the TG and DTG data there were determined the adsorption capacities Figs 4 and 5 of liquid and desorption energy distribution functions using the dependence [28]:

$$-\frac{1}{1-\theta_i} \frac{d\theta_i}{dT} = \frac{v_i}{\beta} \exp\left(-\frac{E_i}{RT}\right) \quad (2)$$

where $T=T_0+\beta t$, θ – degree of surface coverage, v – entropy factor, E_i the desorption energy calculated for each temperature, T_0 and T the initial and given temperatures of desorption, respectively, β the heating rate of the sample, t the time and R the universal gas constant and:

Table 2 Adsorption and structural parameters of the modified alumina samples determined from the nitrogen adsorption isotherms

t_{mod}/h	Sample	$S_{\text{BET}}/\text{m}^2 \text{ g}^{-1}$	$V_{\text{ads}}/\text{m}^3 \text{ g}^{-1}$	$V_{\text{des}}/\text{m}^3 \text{ g}^{-1}$	D_{AV}/nm	$D_{\text{IV-N}_2}$	$D_{\text{fp-AFM}}$	$A_{\text{PR}}/\text{mg g}^{-1}$
2	Al_2O_3 –BSA–Ph–pH 4.9	154.4	0.20	0.19	4.84	2.26		5.44
24	Al_2O_3 –BSA–Ph–pH 4.9	154.2	0.19	0.18	4.69	2.32	–	9.47
2	Al_2O_3 –BSA–Ph–pH 7	157.8	0.21	0.21	4.97	2.30		4.59
24	Al_2O_3 –BSA–Ph–pH 7	156.3	0.20	0.19	4.79	2.27	–	5.21
2	Al_2O_3 –BSA–KCl–pH 4.9	181.04	0.23	0.21	4.56	2.26		3.52
24	Al_2O_3 –BSA–KCl–pH 4.9	183.2	0.23	0.21	4.56	2.27	2.7	11.19
2	Al_2O_3 –BSA–KCl–pH 7	181.0	0.23	0.21	4.61	2.26		3.71
24	Al_2O_3 –BSA–KCl–pH 7	184.1	0.23	0.21	4.57	2.27	2.63	4.98
2	Al_2O_3 –Oval–Ph–pH 4.9	158.1	0.21	0.20	4.85	2.27	–	1.81
2	Al_2O_3 –Oval–Ph–pH 7	155.4	0.21	0.19	4.81	2.25	–	2.79
24	Al_2O_3 –Oval–KCl–pH 7	182.9	0.23	0.20	4.48	2.25	2.68	6.89

t_{mod} – modification time, S_{BET} – specific surface area, V_{BET} – the pore volume, D_{AV} – pore diameter, D_{IV} – volume, D_{fp} – surface fractal dimensions, A_{PR} – amount adsorbed albumin

Table 3 Changes of desorption energy of the liquid from the tested alumina samples

Sample	Benzene				<i>n</i> -octane				Water			
	E_{dp}	$E_{d,max}$	E_{dk}	$Q_{E_{d,max}}$	E_{dp}	$E_{d,max}$	E_{dk}	$Q_{E_{d,max}}$	E_{dp}	$E_{d,max}$	E_{dk}	$Q_{E_{d,max}}$
Al ₂ O ₃	20	28.6	45	9.2	15	27.3	41	3.7	40	52.9	82	16.4
Al ₂ O ₃ -Ph-pH 7-2 h	18	32.4	55	9.6	12	26.6	43	3.4	16	41.7	60	16.3
Al ₂ O ₃ -BSA-Ph-pH 4.9-24 h	21	34.7	53	7.9	12	28.3	46	3.4	17	44.5	70	16.0
Al ₂ O ₃ -BSA-Ph-pH 7-24 h	21	29.9	47	7.9	15	30.1	42	4.5	20	44.8	60	15.7
Al ₂ O ₃ -Oval-Ph-pH 4.9-2 h	20	27.1	39	6.1	13	26.0	38	3.7	24	44.3	55	16.0
Al ₂ O ₃ -Oval-Ph-pH 7-2 h	22	32.6	50	7.3	12	27.5	52	3.7	17	44.7	64	14.8
Al ₂ O ₃ -KCl-pH 4.9-2 h	17	30.8	44	8.4	16	30.1	46	4.4	23	41.7	60	14.8
Al ₂ O ₃ -KCl-pH 4.9-24 h	15	27.9	49	14.7	13	26.1	38	4.0	20	44.4	62	18.7
Al ₂ O ₃ -KCl-pH 7-2 h	19	29.8	50	8.6	9	21.8	33	12.4	23	31.9	41	19.3
Al ₂ O ₃ -BSA-KCl-pH 4.9-2 h	21	37.9	51	19.9	13	28.2	40	4.1	12	22.1	26	15.0
Al ₂ O ₃ -BSA-KCl-pH 4.9-24 h	19	30.9	51	8.8	9	22.2	30	9.9	13	36.0	58	34.0
Al ₂ O ₃ -BSA-KCl-pH 7-24 h	19	35.0	58	10.5	10	18.9	28	2.7	19	47.5	71	15.7
Al ₂ O ₃ -Oval-KCl-pH 4.9-24 h	17	27.4	45	7.0	14	27.8	38	4.2	20	41.6	58	18.8
Al ₂ O ₃ -Oval-KCl-pH 7-24 h	18	31.3	47	9.1	14	26.2	45	3.6	19	46.2	68	20.0

Units: E_{dp} , $E_{d,max}$, E_{dk} – kJ mol⁻¹, $Q_{E_{d,max}}$ – μmol kJ⁻¹

$$\varphi_n(E) = -\frac{d\theta}{dT} \frac{1}{T} \quad (3)$$

Table 3 shows the change of E_d values for individual measurements. The distribution functions differ in shape and range of E_d changes (Fig. 6) which indicates the complex mechanism of this process. $E_{d,max}$ values (of desorption energy in the maximum of distribution function) diminish compared with pure aluminium oxide

($E_{d,max}=52$ kJ mol⁻¹) for water thermodesorption (in the range 40–45 kJ mol⁻¹) for modified surfaces to the increase of a number of active centers of hydrophobic character and weakening of the adsorbent–adsorbate increases. The increase of desorption energy for pure aluminium oxide in the series benzene>octane for acidic solutions and the decrease of $E_{d,max}$ values for octane from neutral solutions were observed.

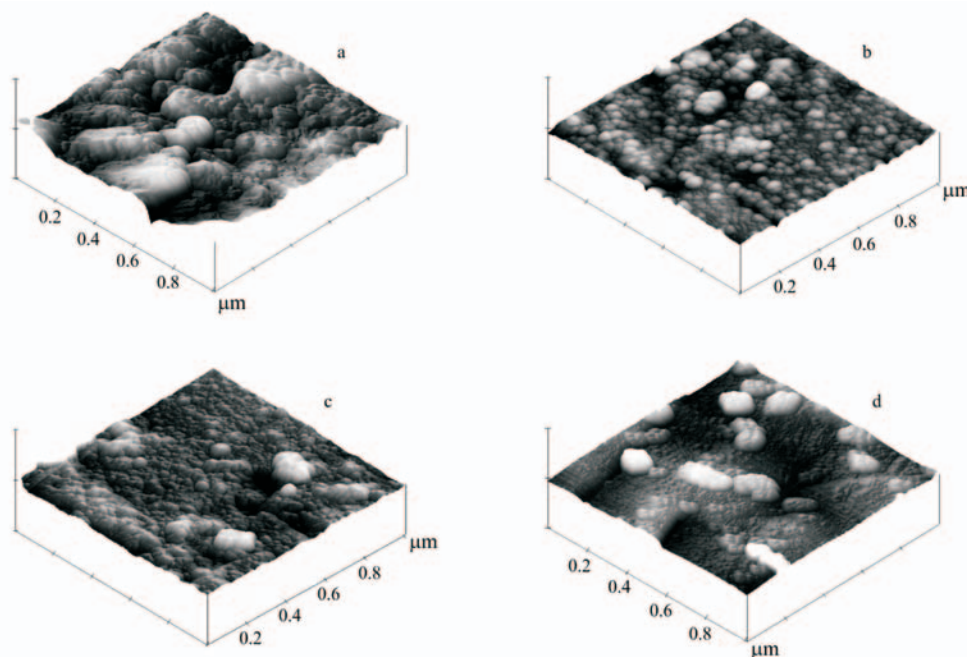


Fig. 2 AFM photographs of the alumina samples modified: a – ovalbumin solution [KCl pH=4.9, 24 h], b – KCl pH 4.9, 24 h, c – phosphate solution, pH 4.9, 24 h, d – BSA solution [KCl pH 4.9, 24 h]

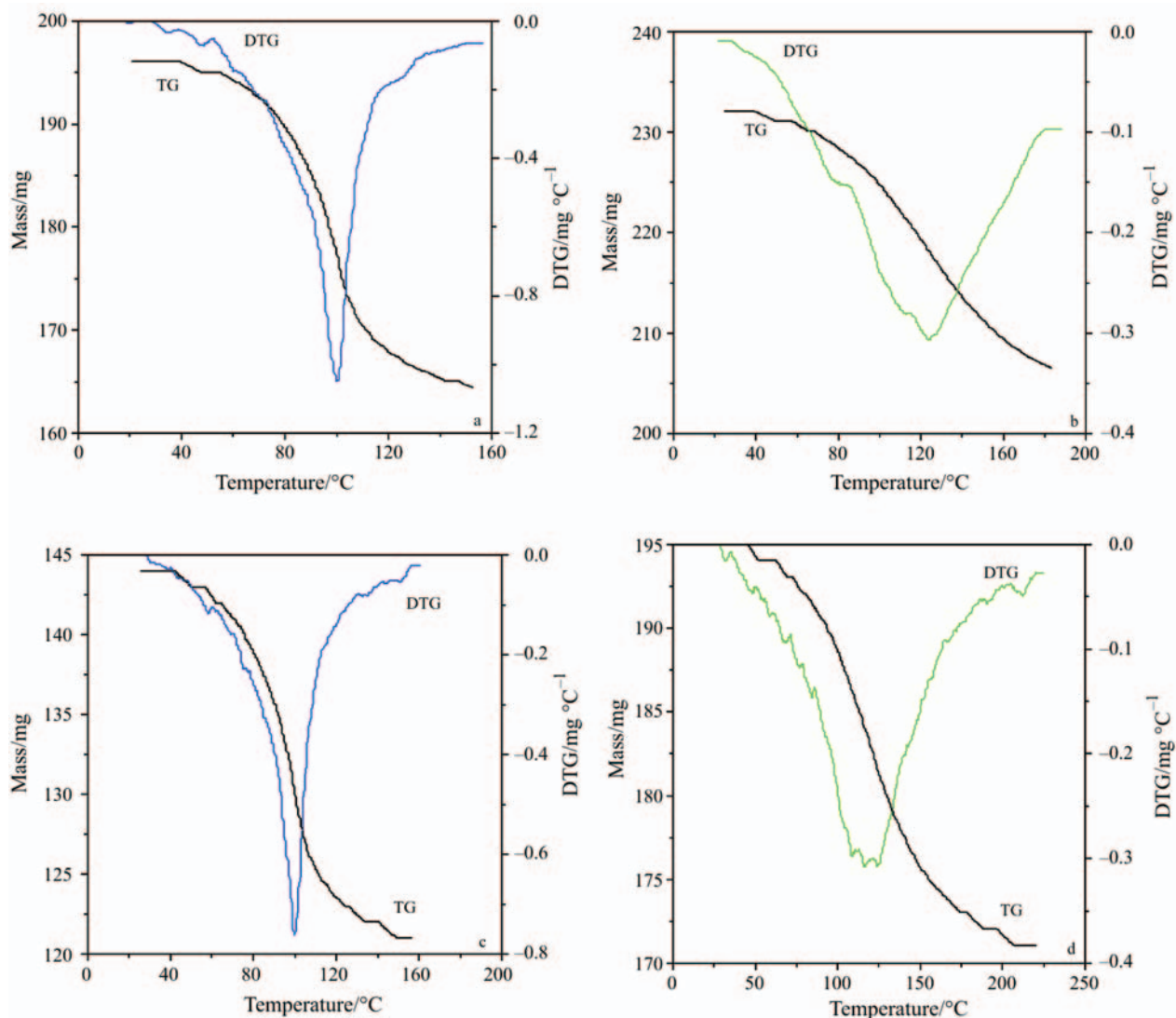


Fig. 3 TG and DTG curves of liquid thermodesorption from the modified and unmodified Al_2O_3 samples; a – Al_2O_3 -water, b – Al_2O_3 -octane, c – Al_2O_3 -24 h-BSA-Ph-pH 4.9-water, d – Al_2O_3 -24 h-BSA-Ph-pH 4.9-octane

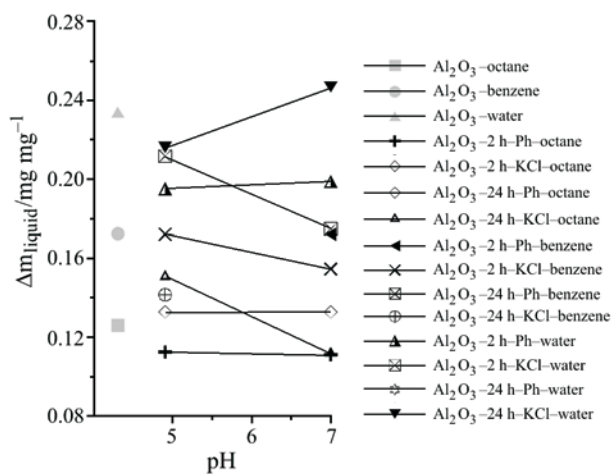


Fig. 4 Dependence of adsorption capacity of liquids on pH of modified Al_2O_3

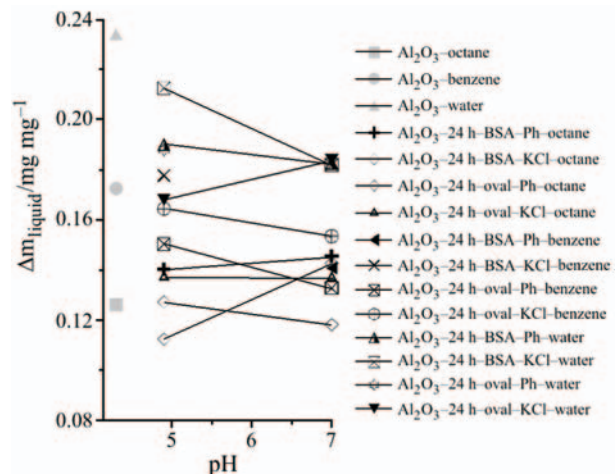


Fig. 5 Dependence of adsorption capacity of liquids on the pH modification of the aluminium oxide on albumins

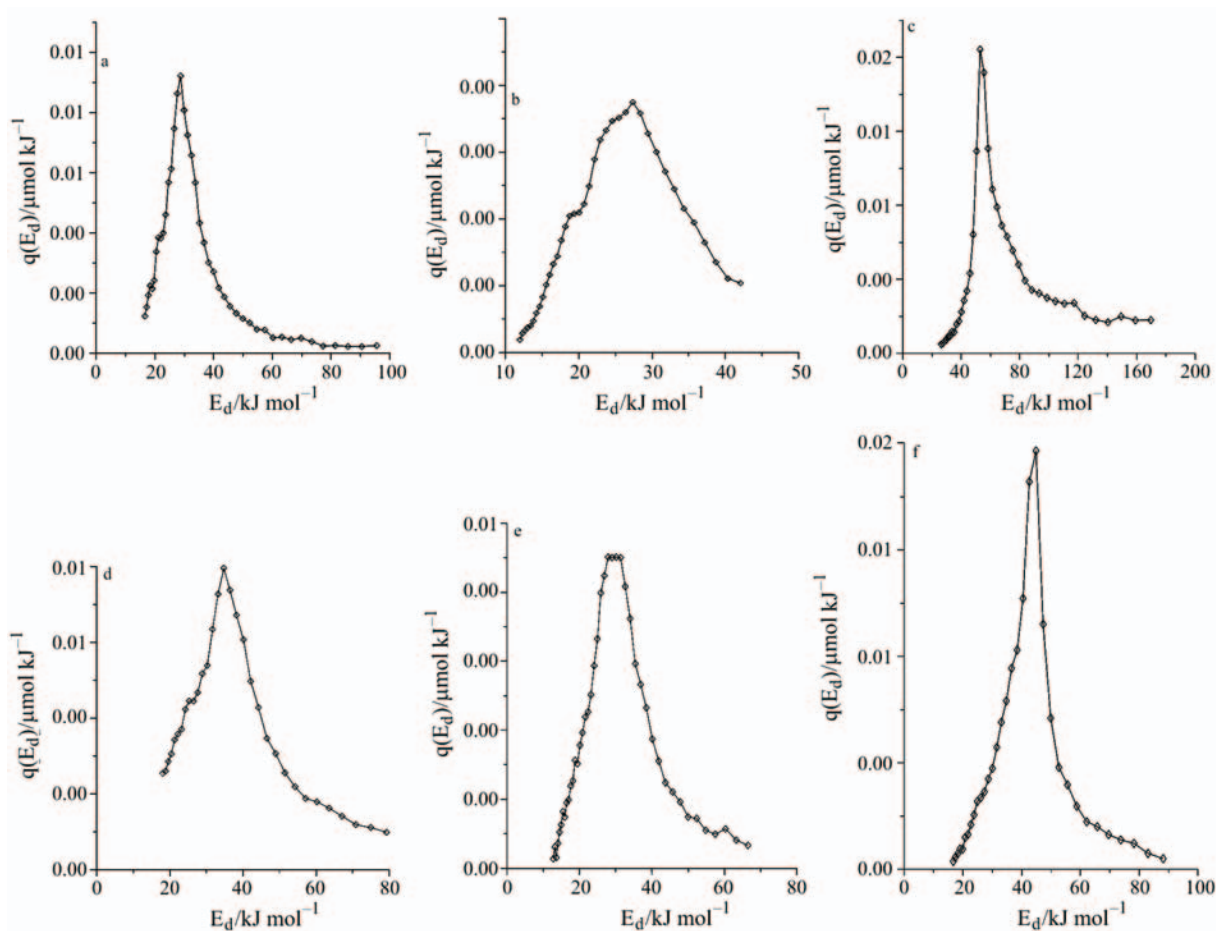


Fig. 6 Energy distribution function of liquid desorption from modified and unmodified Al_2O_3 samples; a – Al_2O_3 –benzene, b – Al_2O_3 –octane, c – Al_2O_3 –water, d – Al_2O_3 –24 h–BSA–Ph–pH 4.9–benzene, e – Al_2O_3 –24 h–BSA–Ph–pH 4.9–octane, f – Al_2O_3 –24 h–BSA–Ph–pH 4.9–water

Conclusions

The process of albumin adsorption is very complicated and depends on many factors: modification time, acidity stabilizer, electrostatic interactions between the adsorbent and the adsorbate as well as type of albumin. In the case of aluminium oxide the effect of albumin adsorption on total heterogeneity of adsorbents is not explicit. On the one hand, the samples modified with albumins showed decrease of surface area with increase of surface coverage with albumin. On the other hand, modifications under the same conditions but without albumin caused similar changes. These effects suggest strong influence of pH of medium on surface properties (due to surface polarization) and competitive co-adsorption of ions on this process.

Acknowledgements

This work was supported financially by the Ministry of Science and Education of Poland, Grant MEiN 3 T09B 113 29.

References

- 1 H. L. Fleming, *Stud. Surf. Sci. Catal.*, 120 (1998) 561.
- 2 S. Joshi and J. Foir, *Ind. Eng. Chem. Fund.*, 3 (1986) 4.
- 3 P. C. Saunders and J. W. Hightower, *J. Phys. Chem.*, 74 (1970) 4323.
- 4 G. Gati and H. Knozinger, *Z. Phys. Chem.*, 78 (1972) 243.
- 5 J. B. Peri, *J. Phys. Chem.*, 69 (1965) 220.
- 6 B. C. Lippens and J. J. Steggerda, *Physical and Chemical Aspects of Adsorbents and Catalysts*, Academic, New York 1970, p. 171.
- 7 R. Fiedorow, R. Leaute and I. G. Dalla Lana, *J. Catal.*, 85 (1984) 339.
- 8 J. Berk, *Przem. Chem.*, 51 (1972) 607.
- 9 G. A. Parks, *Chem. Rev.*, 65 (1965) 177.
- 10 C. P. Huang and W. Stumm, *J. Colloid Interface Sci.*, 43 (1973) 409.
- 11 L. Wang and W. K. Hall, *J. Catal.*, 66 (1981) 251.
- 12 J. A. Davis and J. O. Leckie, *J. Colloid Interface Sci.*, 74 (1980) 32.
- 13 C. A. Haynes and W. Norde, *Colloids Surf., B*, 2 (1994) 517.
- 14 A. Sadana, *Chem. Rev.*, 92 (1992) 1799.
- 15 P. M. Claesson, E. Blomberg, J. C. Fröberg, T. Nylander and T. Arnebrant, *Adv. Colloid Interface Sci.*, 57 (1995) 161.
- 16 S. Oscarsson, *J. Chromatogr. B*, 699 (1997) 117.

- 17 H. Larsericsdotter, S. Oscarsson and J. Buijs, *J. Colloid Interface Sci.*, 289 (2005) 26.
 - 18 M. M. Bradford, *Anal. Biochem.*, 72 (1976) 248.
 - 19 O. H. Lowry, N. J. Rosbrough, A. L. Farr and R. J. Randall, *J. Biol. Chem.*, 193 (1951) 265.
 - 20 G. M. Oostra, N. S. Mathewson and G. N. Catrivas, *Anal. Biochem.*, 89 (1978) 31.
 - 21 N. J. Greenfield, *Trends Anal. Chem.*, 18 (1999) 236.
 - 22 S. M. Kelly and N. C. Price, *Biochim. Biophys. Acta*, 1338 (1997) 161.
 - 23 F. Parker, *Applications of Infrared, Raman and Resonance Raman Spectroscopy in Biochemistry*, Plenum Press, New York 1983.
 - 24 T. Chen and D. M. Oakley, *Thermochim. Acta*, 248 (1995) 229.
 - 25 H. Urano and S. Fukuzaki, *J. Colloid Interface Sci.*, 252 (2002) 284.
 - 26 D. Sarkar and D. K. Chattoraj, *J. Colloid Interface Sci.*, 178 (1996) 606.
 - 27 B. M. Kats and V. V. Kutarov, *Langmuir*, 12 (1996) 2762.
 - 28 P. Staszczuk, D. Sternik and V. V. Kutarov, *J. Therm. Anal. Cal.*, 69 (2003) 23.
-

DOI: 10.1007/s10973-006-7580-8